On the non monotonic recess effect on coaxial atomization

Arnaud DUNAND, Jean-Louis CARREAU and Francis ROGER

Laboratoire de Combustion et Détonique CNRS UPR 9028
University of POITIERS
ENSMA, 1 avenue Clément Ader, BP 40109
86961 Futuroscope Chasseneuil Cedex
Phone : 05 49 49 83 05, Fax : 05 49 49 82 91, e-mail : dunand@lcd.ensma.fr

Liquid tube recess (R/D_i) according to the injector exit plane is widely used in injection elements for technical applications. Previous studies dealing with effect of recess revealed the apparition of a non-monotonic behaviour. In order to obtain complementary information, this analysis highlights a new laser technique, based on imaging diagnostic, enabling to size large liquid structures without spherical shape condition. This study deals also with effect of chamber pressure (P_c) - tests were conducted at pressures equal to 0.1 and 0.9 MPa and with spray mixing with ambient air. The main results were: set-up of a reliable and promising granulometric technique, which information are complementary of PDA ones and confirms previous interpretations on the recess effect, poor secondary atomization is achieved for large values of R/D_i but it was compensated with high mixing compared with low values of R/D_i. Pressure effect seems to be the same for all recess distance tested, spatially reducing potential atomization location and has no influence on the non-monotonic effect. Choice of recommended recess value is guided by many parameters as operating conditions or atomization/mixing compromise.

1. Introduction

It is well known that recessing the liquid tube of an injection element improves cryogenic flame stabilization and therefore rocket engine reliability. Since preliminary studies [1], cryotechnic engines are equipped with coaxial injectors provided with recess. Nevertheless, only few analyses have been carried out in order to complement them, and above all, results provided are most of the time inconsistent. One of the main facts is the appearance of a non-monotonic effect according to the value of the recess distance [2,3]. Recently [4], an analysis, based on the gas/liquid interaction inside the injection element, interprets the occurrence of these different behaviours. It seems important to adapt the distance recess with operating conditions and according to what is researched. Therefore, present analysis highlights some points like confinement phenomenon consequences and atomization/mixing compromise when a recess is using. This study is achieved by means of a new laser diagnostic taking into account large liquid droplet population and an experimental study of entrained surrounding air.

2. Experimental setup and operating conditions

The experimental setup, called JETCOAP, allows measurements in the pressure range of 0.1 MPa to 1 MPa with a motorised two-dimension displacement system of the injector (precision 10 µm). We use five coaxial injectors (figure 1) with the same geometry: 2.1 and 3.6 mm inner diameter respectively for the liquid (D_i) and the gas (D_{g0}) tube, the recess only varying between 0 and 4 mm, with a 1 mm gap for each injector (R/D_i = 0, 0.48, 0.95, 1.43 and 1.90). In order to characterize the dilute spray region, in terms of velocity and diameter of the spherical liquid droplet distributions, we use a phase Doppler technique. This laser diagnostic is completed by a new one, developed at the laboratory [5], in order to increase the measurement range and take into account the non-spherical particles.

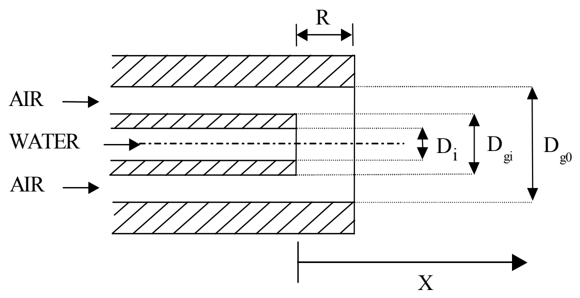

Fig. 1: Schematic of the injector and main dimensions.

2.1. Phase Doppler Analyzer

Quantitative information on the spray were obtained with a two dimensional Phase Doppler Analyzer device [6], which enabled local simultaneous measurements of the temporally averaged droplet size and axial velocity distributions within the spray. The optical configuration for these tests included an Argon laser (λ = 532 nm) coupled with a transmitter fitted with a 600 mm focal length lens and a receiver oriented at 60° from the forward direction of the transmitter optical axis. This optical configuration enables velocity measurements from – 25 to 125 m/s and particles sizing up to 145 µm. Number of samples validated at each acquisition position is 5000, in order to have a good statistical representation, within a time limit set at 60 s. For this study, we concentrate on the Sauter Mean Diameter (D_{32}) evolutions because they are representative of vaporization on combustion time ratio [7] and are widely use for numerical code comparisons.

2.2. Laser sizing technique

One of the main limitations of the classical PDA technique is the relatively restrained droplet size range. Nevertheless, in fiber type breakup atomization, as encountered in our experimental configuration [8], large liquid structures remain in dilute spray region. These structures cannot be validated by the PDA because of their size or their non-spherical shape. A large proportion of the liquid fraction is contained in these structures, it is then very important to obtain information on them.

The new granulometric laser technique is based on a Particle Tracking Velocimetry bench developed at the laboratory, called high-resolution displacement technique. This technique lies on detection and sizing of particles from tomographic images. In order to obtain two-phase jet structure (figure 2), we use mie-scattering technique, also known as tomography. Light source, a Nd-Yag laser (λ = 532 nm), illuminates directly the liquid jet. Pulse duration is about 20 ns and therefore spray structures are frozen. By using two lenses, one for the convergence and the other to make the sheet, the laser sheet dimensions are 500 µm X 10 cm X 10 cm, dimensions sufficient for equal energy distribution considerations [8]. A CCD camera (8 bits) with high resolution (1300 X 1024 pixels^2) composes the acquisition system. In order to prevent CCD sensor saturation, a liquid crystal obturator with low transmission coefficient (30 %) and a delay generator Standford to regulate laser emission energy are used [9]. Quality of obtained images is very good (figure 3) permitting numerical treatments and structure detection and sizing.

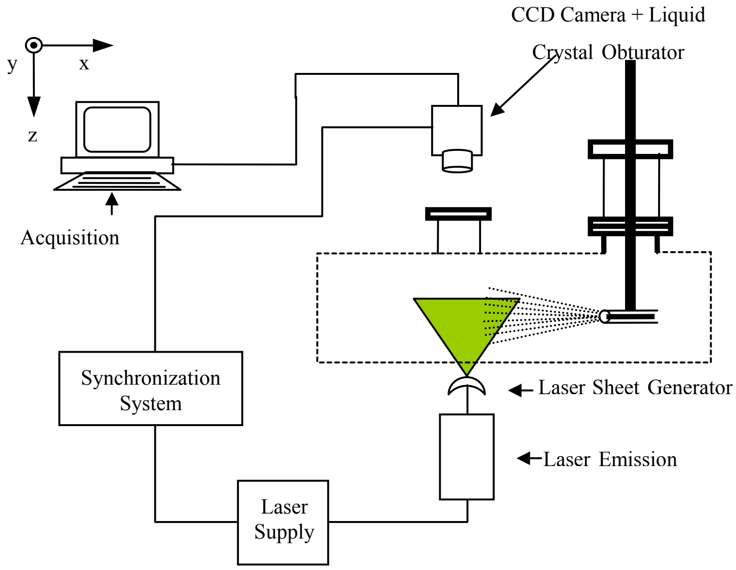

Fig. 2: Imaging technique system.

Detection and sizing algorithm is well documented in [5]. A pixel is considered signal if its intensity is three times its root mean square grey level value. Sizing method detects neighbours pixel intensity of the signal pixel and determines if light repartition is a gaussian type. If it is the case, a gaussian function is interpolated and structure size corresponds to three times the width at half height of this function. This numerical algorithm is proceeded in steamwise and in transversal direction and equivalent size of the detected object is given by the square root of the product of these two distances. This algorithm was validated thanks to synthetic images [9].

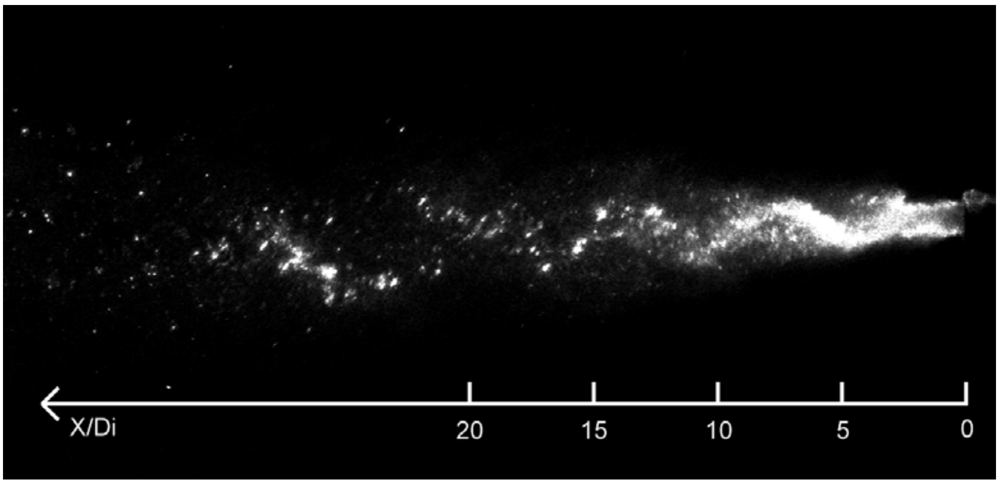

Fig. 3: Instantaneous spray tomography at atmospheric pressure and $R/D_i = 0$

In order to link calculated equivalent diameter with the real droplet diameter, we has to determine a calibration factor. As theoretical approach appearing extremely difficult [10], we obtain this factor by means of a monodisperse piezoelectric injector [11] in the same conditions as for the spray tomography. A typical mie-scattering image of the monodisperse spray is displayed on figure 4. Relation between droplet size and calculated diffusion spot are represented on figure 5.

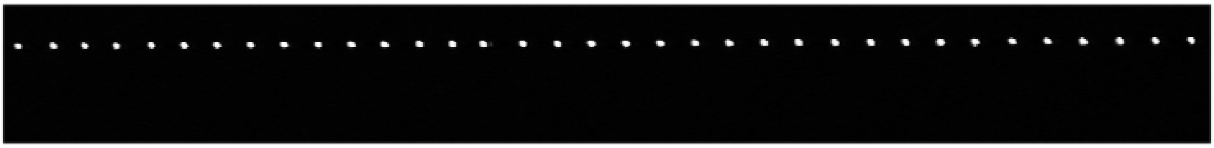

Fig. 4: Instantaneous tomography of the monodisperse spray

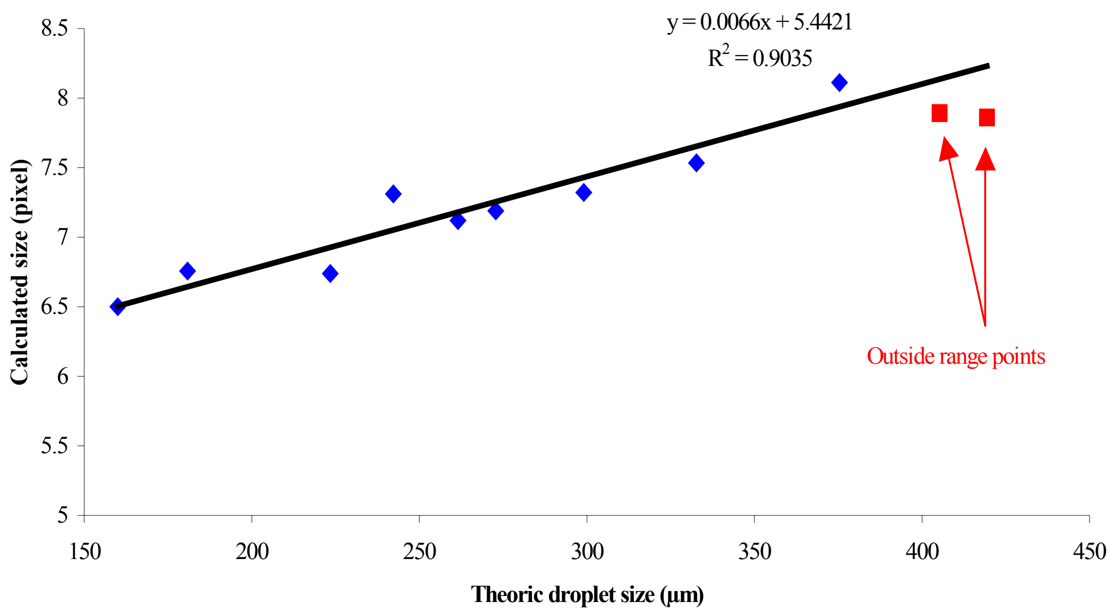

Fig. 5: Calculated object size evolution with calibrated droplet size

This illustration enables to determine possible range of this diagnostic. Between 160 and 380 µm, the relation corresponds to a linear evolution of the calculated size with the droplet real size. After 380 µm, calculated size stays nearly constant revealing difficulties for the sizing algorithm to determine structure size larger than 380 µm. Below 160 µm, results are very inconsistent. Therefore, the range of sizing for this diagnostic is comprised between 160 and 380 µm, we can note that this scale is complementary with the PDA one.

Operating conditions are summarized in the following table (Table 1) where U_l, U_{gi}, ρ_{gi}, m_{gi}, We_{gi}, J, Re are respectively the liquid jet velocity, the gas jet velocity, the gas steam density and mass flow rate, the Weber number $\rho_{gi}(U_{gi}-U_l)^2/\sigma$, the momentum flux ratio $(\rho_{gi}U_{gi}^2/\rho_l U_l^2)$ and the liquid Reynolds number $(\rho_l U_l D_i/\mu_l)$.

Pc (MPa)	U_l (m/s)	U_{gi} (m/s)	ρ_{gi} (kg/m^3)	m_{gi} (g/s)	We_{gi}	J	Re
0.1	2.5	175	1.6	1.73	1300	8	5250
0.9	2.5	67	11.2	3.93	1300	8	5250

Table 1: Operating conditions

For this study, experimental conditions are restricted to the analysis of recess and chamber pressure influences and simulating fluids are water and air. Liquid jet velocity for its part stays constant and equals to 2.5 m/s.

3. Results and discussion

Radial evolutions of mean axial droplet velocities for constant value of J and two surrounding air pressure, figure 6, show quite contrasted behaviours of the spray according to recess value as, for example, the over speed for $R/D_i = 1.90$ and the very low velocity for $R/D_i = 1.43$. Spray development for $R/D_i = 0.48$ and 0.95 seems to be the same. Recess effect is located on the near spray axis region with an overall increase of the droplet velocities and therefore an improved atomization. Chamber pressure seems to spatially decrease the recess effect but have no influence on the non-monotonic trend, as all the observed behaviours are still presents. At 0.9 MPa, for all the recess values, velocity profiles are nearly self establish, synonymous of a precocious stop of secondary atomization processes due to a diminution of gas injection velocity in order to maintain the momentum flux constant.

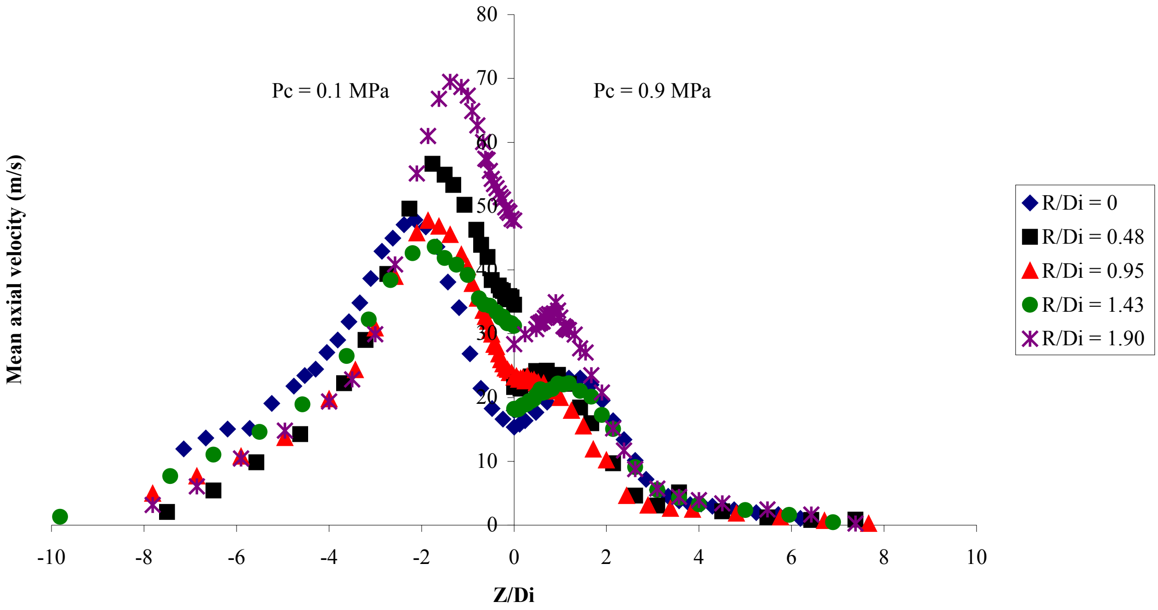

Fig. 6: Radial evolutions of mean velocity for $X/D_i = 10$.

Introducing a recess inside a coaxial injector enables a better atomization and a significant diminution of droplet diameters at 0.1 MPa, as illustrated on figure 7. But this observation is only verified on the spray axis. Actually at the spray periphery, two behaviours according to R/D_i value occurred. For large value of the recess ($R/D_i = 1.43$ and 1.90), secondary atomization is precociously finished with radial distance. For thee recess values, on spray axis, one can see that droplet diameters for $R/D_i = 1.43$ are higher than for $R/D_i = 1.90$. We explain this difference later in the paper. For the other value of the recess distance, secondary atomization is still present with apparition of small diameter on the edge of the spray. At jet periphery, due to a large dispersion of the spray or a lack of velocity differential between droplets and annular gas steam, D_{32} are higher for $R/D_i = 1.43$ and 1.90. This situation is nearly the same at 0.9 MPa. As observed for the radial evolution of the mean axial velocity, atomization is radially rapidly finished because of the reduced gas injection velocity. Recess have the same impact as atomization is only still visible the injection element without recess due to precocious momentum transfer in the near field of the spray [8]. At high chamber pressure, coalescence phenomenon is favoured [12], as D_{32} increase significantly at spray periphery. This behaviour seems to be amplified for large values of R/D_i, reinforcing the idea of a delayed secondary atomization for these recess distance.

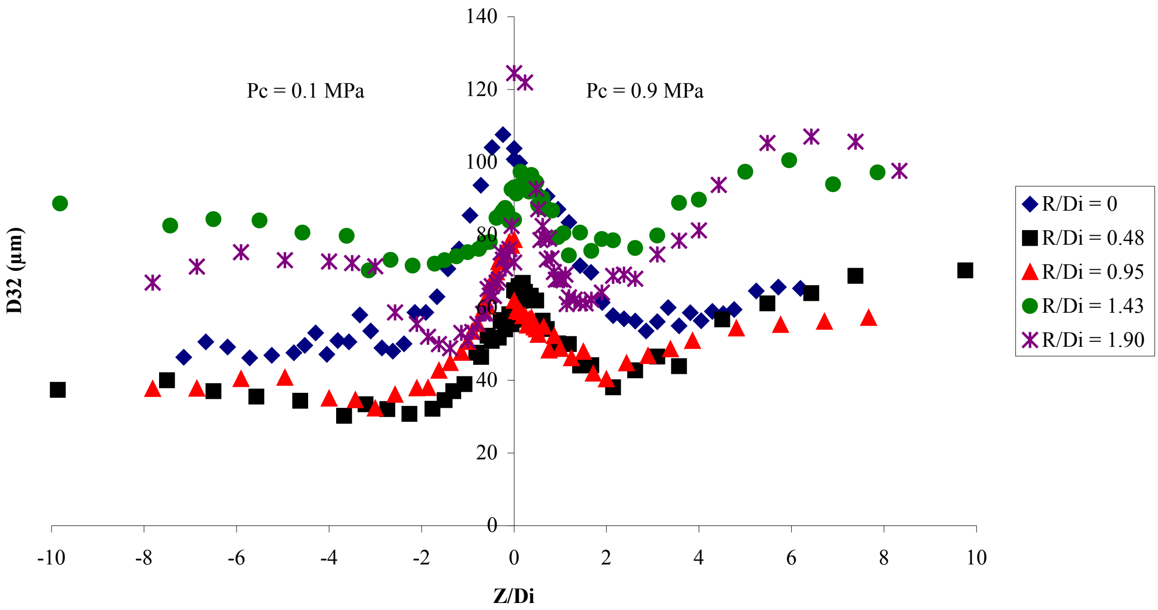

Fig. 7: Radial evolutions of Sauter mean diameter for $X/D_i = 10$.

Another interrogation concerning the non monotonic recess effect corresponds to results obtained by [4] and in this study, that is to say unexplained great differences of Sauter mean diameter between $R/D_i = 1.43$ and 1.90 not in agreement with confinement phenomenon engenders by the over speed observed for $R/D_i = 1.90$. Fist analysis [13] revealed disparity between droplet populations for these two recess distances, with a homogenous repartition for $R/D_i = 1.43$ and small droplet size in majority for $R/D_i = 1.90$. Thanks to the new laser sizing technique, we now obtain information on large size liquid structures spherical or not, which in this case are not validated by the Phase Doppler system. Figure 8 illustrates droplet repartition histogram and we can observe large liquid cluster presence for $R/D_i = 1.90$, which was not take into account with the PDA technique. So, we can say that, although D_{32} obtained by PDA are small, spray quality for $R/D_i = 1.90$ injector is very poor, which is good agreement with previous interpretations [8]. The new diagnostic enables then to favourably complements results obtained by PDA to quantify atomization processes and reinforces previous interpretations [4].

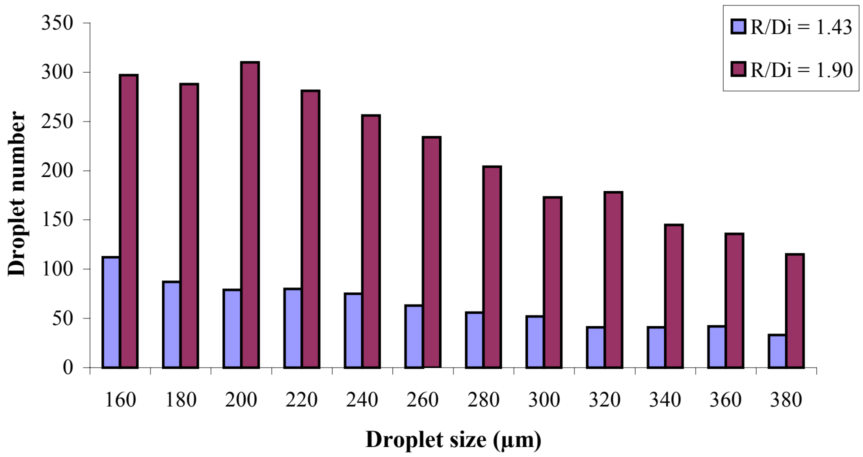

Fig. 8: Droplet size histogram at atmospheric pressure and $X/D_i = 10$.

These evolutions show that secondary atomization is better for low value of recess distance (R/D_i = 0.48 and 0.95). In order to quantify another useful information of atomization process, we have study the entrainment rate of each spray to obtain the mixing capacity of the two-phase flow according to recess value. By analogy with [14], entrained gas mass flow rate is determined by integration of the radial profile of axial gas velocity on the jet section (Eq. 1). Local gas velocity was determined by velocity of the droplet which size is below 15 µm, which follow preferentially the gas phase steam [12].

$$\frac{\dot{m}}{\dot{m}_{inj}} = \frac{2\,\pi\,\rho \int_0^{r_\infty} r\,U(r)\,dr}{2\,\pi\,r^2\,\rho_{gi}\,U_{gi}} \qquad (1)$$

At first sight, one can observe a linear evolution of the entrained gas mass flux with axial distance on figure 9. This evolution is in good agreement with other studies in monophasic [15] or two-phase conditions [16]. For an injector without recess, the coefficient is nearly equals to 0.25, which is lower than the well-known value of 0.32 [15]. But, for a two-phase jet, it has been proved that droplet presence reduces turbulence stress and consequently entrainment rate [17]. Figure 9 shows an increase of entrained surrounding gas with recess distance. We note that, at atmospheric pressure and in the intermediate field of the spray, large values of R/D_i (R/D_i = 1.43 and 1.90) induce great enhancement of entrainment. Then, we can say that large values of recess compensate its lack of secondary atomization processes by a great mixing with the ambient medium. Nevertheless, for a chamber pressure of 0.9 MPa, entrained air induced by R/D_i = 0.48 and 0.95 is comparable to the one of large value of recess. This trend derives from a higher interfacial velocity because for these injectors, annular gas jet doesn't lose too much kinetic energy [8]. Moreover, mixing layer development stop precociously for large values of recess.

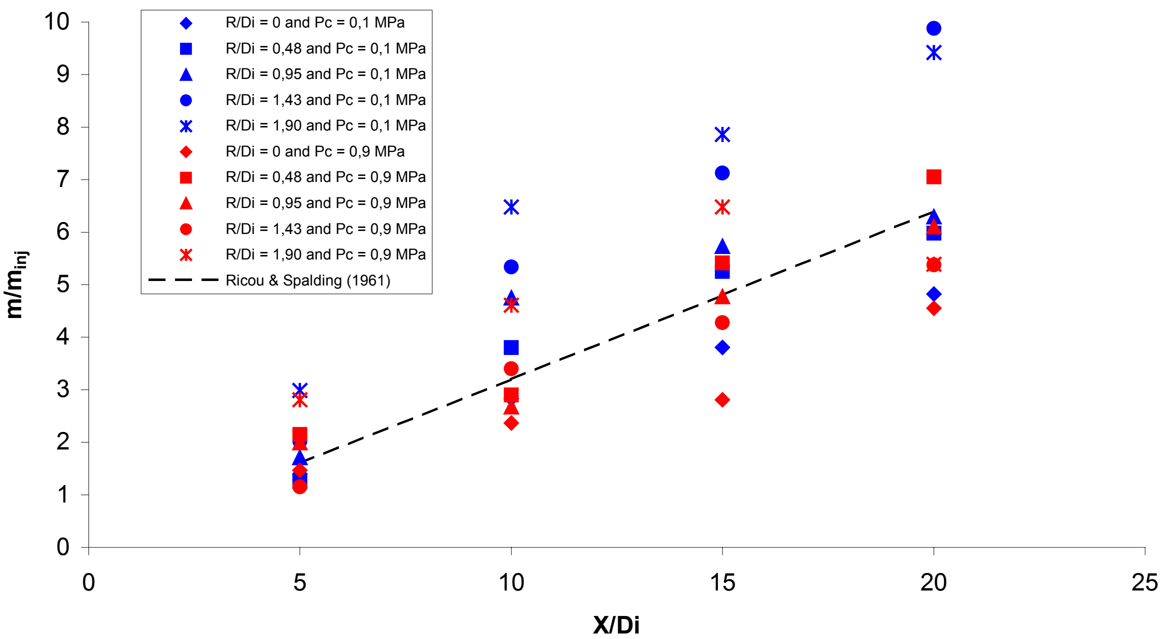

Fig. 9: Axial evolution of entrained mass flow rate.

4. Conclusion

This study gives complementary information on non-monotonic behaviours in order to enhance the cryogenic flame stabilization. New sizing technique gives crucial information in order to quantify atomization quality and can be use in complementary of the PDA diagnostic. Choice of the best recess value seems to mainly depend on injection, surrounding conditions and goal we looked for, as a lot of trends must be taken into account. Actually, at atmospheric pressure, in terms of atomization it was clear that small values of recess are recommended but if mixing is required then large values of R/D_i must be used. Nevertheless, at high surrounding pressure, small values of recess distance are always advocated. Chamber pressure does not have any influence on the non-monotonic effect appearance and seems independent of the recess value with a reduction of potential atomization location and slightly improvement of secondary atomization.

Acknowledgements
The authors acknowledge financial support from CNES, SNECMA Moteurs, the MENESR France and Ms Lavergne G and Biscos Y for the monodisperse injector lending.

Nomenclature

D_i	Nozzle diameter for the liquid
D_{g0}	Nozzle diameter for the gas
D_{32}	Sauter Mean Diameter
J	Momentum flux
m	Mass flow rate
P_c	Chamber pressure
R	Recess value
r	Radial distance
U	Velocity
X	Axial distance from liquid tube exit
Z	Radial distance
ρ	Density
σ	Surface tension
λ	Wavelength

<u>Subscripts</u>

c	chamber
g	gas
i or ing	injection
l	liquid

References

[1] Wanhainen J. P., Parish H. C., Conrad E. W., 1966, *NASA Technical notes*, NASA TN D-3373.
[2] Burick, R.J., 1972, *Journal of Spacecraft and Rockets*, **9**, No. 5, 326-331.
[3] Tripathi A., Juniper M., Scouflaire P., Durox D., Rolon C., Candel S., 1999, *AIAA Paper 99-2490*
[4] Dunand A., Carreau J.L., Guyot L., Prévost L., Roger F., 2001**,** *ILASS Europe 2001*.
[5] Susset A., Most J.M., Honoré D., 2002, *8ème Congrès de Francophone de Vélocimétrie Laser*.
[6] Bachalo W.D., 1994, *Int. J. Multiphase flow*, **20**, 261-295.
[7] Lefebvre A.H., 1989**,** ed. Hemisphere Publishing Corporation.
[8] Dunand A., 2002, *PhD. Thesis*, University of Poitiers.
[9] Susset A., 2002, *PhD. Thesis*, University of Poitiers.
[10] Gouesbet G., Gréhan G., 2000, *Atomization and Sprays*, **10**, 277-335.
[11] Virepinte J.F., Ravel O., Biscos Y., Lavergne G., Magre P., Farre J., 2001, *Combustion*, **1**, n°3, 178-201.
[12] Prévost L., Carreau J-L., Roger F., 2000, *ICLASS 2000*, Pasadena.
[13] Dunand A., Guyot L., Carreau J.L., Prévost L., Roger F., 2000, *7ème congrès francophone de vélocimétrie laser*.
[14] Crow S.C., Champagne F.H., 1971, *J. Fluid Mech.,* **48**, 547-591.
[15] Ricou P.P., Spalding D.B., 1961, *J. Fluid. Mech.,* **11**, n°21.
[16] Ferrand V., Bazile R., Borée J., Charnay G., 2000, *ICLASS 2000*, Pasadena.
[17] Field M.A., 1963, *The British Coal Utilization Research Association*, No 273.